Materials Science and Engineering A 528 (2011) 1602–1607

Contents lists available at ScienceDirect

Materials Science and Engineering A

journal homepage: www.elsevier.com/locate/msea

Fatigue crack growth behavior of titanium foams for medical applications

Sadaf Kashef[a,*], Alireza Asgari[b], Timothy B. Hilditch[b], Wenyi Yan[c], Vijay K. Goel[d], Peter D. Hodgson[a]

[a] Institute for Technology Research and Innovation, Deakin University, Pigdons Road, Waurn Ponds, Victoria 3217, Australia
[b] School of Engineering, Deakin University, Waurn Ponds, Victoria 3217, Australia
[c] Department of Mechanical and Aerospace Engineering, Monash University, Clayton, Victoria 3800, Australia
[d] Engineering Center for Orthopaedic Research Excellence, University of Toledo, Toledo, OH 43606, USA

ARTICLE INFO

Article history:
Received 24 September 2010
Received in revised form 21 October 2010
Accepted 5 November 2010

Keywords:
Titanium
Foam
Fatigue crack growth
Crack bridging
Crack closure

ABSTRACT

There is an urgent need to understand the failure behavior of titanium foams because of their promising application as load-bearing implant materials in biomedical applications. Following our recent study on fracture toughness of titanium foams [1], this paper investigates the mode I fatigue crack propagation in 60% porous open pore titanium foams both with and without solid coated surface. Fatigue crack propagation tests were performed on compact tension specimens at load ratios of $R = 0.1$ and $R = 0.5$ and the fracture surfaces were examined using scanning electron microscopy. The crack growth rate, da/dN, versus the stress intensity factor range, ΔK, curves were measured and compared using two different techniques; image processing and compliance methods. The crack extension rates were well described by ΔK, using the Paris-power law approach. Coated and non-coated titanium foams with 60% porosity had a significantly higher Paris exponent than solid titanium, which can be explained by crack closure and crack bridging. It was also shown that the fatigue crack grows along the centerline, following the weakest path throughout the foam. The results obtained from this work provide important information for evaluating the structural integrity of porous titanium components in the future biomedical applications.

1. Introduction

Intensive physical activity can lead to stress fracture or micro cracks in load-bearing bones and joints such as the human hip and knee [2]. These fractures are the result of continued repetitive or cyclic fatigue loading [3,4], and damage leading to failure may develop over numerous years. As such, the cyclic fatigue loading properties of biomaterials used for bone replacement is an important consideration.

In recent years, new manufacturing processes and improvements in quality have made foam materials an interesting option for biomedical applications, particularly in load bearing functions such as hip and knee joint replacements. Foam materials offer significant advantages compared to solid materials as the porosity can be varied to match the strength and stiffness of the surrounding bone to minimize stress-shielding [5], as well as the porosity allowing ingrowth of tissue into the implant [5].

Numerous studies have been done on the mechanical properties of metal foams used in industries other than biomedical engineering [6]. For instance, Motz et al. [6], Zettl et al. [7], Olurin et al. [8], and McCullough et al. [9] have investigated fracture mechanics and fatigue properties of different aluminum foams. Alternatively, there are few studies [10–19] on the mechanical properties of titanium foams. For instance, Imwinkelried [17] carried out static compression, cyclic compression, bending, tension, and torsion tests on titanium foam, while Teoh et al. [18] have investigated the effect of pore sizes and cholesterol lipid solution on fracture toughness of pure titanium foam. Pore sizes in the pure titanium samples ranged from 25 μm to 103 μm with porosity of 8.5–35% and it was discovered that the fracture toughness of samples with smaller pore sizes was twice the fracture toughness values of samples with larger pore sizes [18].

While the high cycle fatigue properties of titanium foams have been studied (S–N approach) [17], to-date there are no studies on the fracture mechanics of highly porous titanium foams. As foam structures often have inherent flaws, there is usually no crack initiation stage. Thus, use of S–N approach, which typically incorporates initiation of a crack, is not practical. A realistic way to investigate foam materials is to examine the number of cycles needed to propagate these inherent flaws to failure. Fracture mechanics or damage-tolerant method is usually used for such predictions. For fatigue crack growth (FCG) analysis, the number of cycles needed for a crack to grow sub-critically to a critical size is calculated from information relating the crack velocity to the mechanical driving force, and the stress intensity factor, K [20]. Studying the crack

* Corresponding author. Fax: +61 3 5227 1103.
E-mail address: skas@deakin.edu.au (S. Kashef).

0921-5093/$ – see front matter © 2010 Elsevier B.V. All rights reserved.
doi:10.1016/j.msea.2010.11.024

Nomenclature

a	crack length
C	Paris law coefficient
da/dN	crack growth rate
FCG	fatigue crack growth
ΔK	stress intensity factor range
ΔK_{th}	fatigue crack growth threshold
m	Paris law exponent
N	number of cycles
ν	Poisson's ratio

growth of titanium foam will examine whether they are compatible for biomedical implantations.

In this study, the mechanical properties of pure titanium foams with 60% porosity (relative density of 0.40) have been examined by using mode I of crack growth testing, and the results are compared against a range of skeletal components. Foams were manufactured using the space-holder method [21] both with and without a solid coating. Typically, low porous metals have higher stiffness and strength than high porous metals; but do not have space for bone ingrowth [22]. Conversely, high porous metals have more space for bone regeneration with lower stiffness and strength. A good implant material should have both permeability and strength. For growth of bone tissue into the pores and connectivity of macropores, the material must have at least 55% porosity [15,23]. Titanium foam with 60% porosity was chosen because this porosity not only is suitable for bone ingrowth but its strength and toughness is shown to be appropriate for biomedical applications [1,17,21]. The objective of this research is to understand the mechanisms of fatigue crack propagation in titanium foams and to compare these results with the fatigue data on the bone, dentine, and current implant materials from literature.

2. Experimental procedures

2.1. Material and specimen preparation

Commercially available 99.9% purity titanium powder (Atlantic Equipment Engineers, USA) with an average particle size of 45 μm and irregular morphology was used. To produce open porous titanium material, the space holder method was used [24]. This method has been applied by Teoh et al. [18], Wen et al. [5], Imwinkelried [17], and Kashef et al. [21]. In this process, the fine titanium powder was mixed with the space holder substance and pressed at room temperature under 200 MPa pressure. The space holder was removed by heat treatment at 100 °C for 10 h and the remaining titanium sintered at 1120 °C for 7 h in a vacuum furnace [21]. The purity of the titanium foam is considered to be still above 99.0% after sintering. Ammonium bicarbonate powder, NH_4HCO_3 (Sigma–Aldrich) with 99.0% purity was used as space holder material. The angular-shaped particles were obtained with 500–800 μm size by sieving. The spacer material was chosen such that it decomposes completely at a low temperature. The weight ratio of the titanium powder to spacer was chosen to be 60–40% to obtain the desired porosity.

2.2. Fatigue crack growth test

The compact tension (CT) titanium foam samples with dimensions of 31.25 mm × 30 mm × 6 mm (Fig. 1) were machined from larger pieces of 55 mm × 50 mm × 6 mm and then pre-cracked as explained in ASTM E647-08, the standard test method for measurement of fatigue crack growth rates. Two groups of samples were

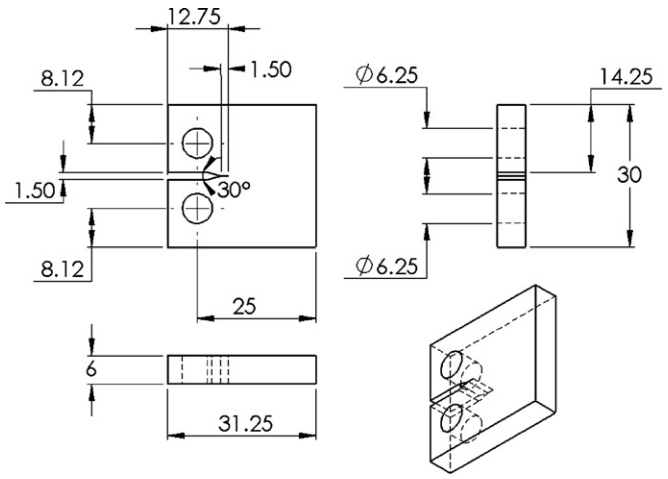

Fig. 1. Schematic of a titanium CT specimen.

prepared: one with a thin solid coat and the other without any coating. For the coated samples, a thin surface layer of solid titanium was allowed to form around the sample by the heat dissipated from a regular cutting process. The solid film of titanium is simply created by localized melting of the sample surface during machining. The average thickness of this solid titanium film was 0.5 mm. The purpose of studying the fatigue crack growth rate of the porous samples with solid coating is to provide a comparison basis for the analyses of fatigue crack growth rate in the porous samples without any coating. However, the preparation method used in this paper to create the solid coated surface is only limited to simple plate and regular surfaces and cannot be used for complex shapes. Samples without coating were wire cut with the temperature controlled so that no melting, hence surface layer, was introduced to the surface.

FCG testing was carried out at room temperature on a MTS servo-hydraulic test machine (MTS 858) in accordance with ASTM E647-08. Tests were conducted at load ratios (minimum load/maximum load) of $R = 0.1$ and $R = 0.5$ and frequency of 40 Hz. It has been shown that the correlation of experimental values for positive ratio of $0 \leq R \leq 1$ is better than for R less than zero [25] and thus the load ratios of $R > 0$ were chosen for this study. Initially, the yield load of the samples was determined by putting samples under tension. To find out the maximum allowable cyclic loads, a set of sacrificed samples were used, which were cyclically loaded near the ultimate tensile strength (UTS). The cyclic failure loads of the sacrificed samples were found to be less than the UTS. Then, the maximum allowable load was determined at 5% below the cyclic failure loads of the sacrificed samples. As a result, the maximum load of 200 N was applied for samples without a solid coated surface while a maximum load of 350 N was applied for samples with solid coated surface. At the final fracture stage, the frequency was reduced to 10 Hz to obtain more data. As stated in standard, a single specimen was enough to get the desired data and at least five samples for each material were tested.

2.3. Measurement of crack growth

Measurement of crack growth was done with the following two techniques:

- Image processing.
- Compliance technique.

Digital images of the samples' surfaces were taken during the FCG testing. Camera's speed was about 3 fps (frames per second) up to the highest speed of 6 fps. Photographic grids were used on

digital images of crack tip growth that were taken from both sides of the samples without interrupting the test. The average of crack length on each side of the sample was used as the crack size from image processing technique. Each measurement was carried out at least three times. By image processing technique, the crack size is measured as a function of elapsed fatigue cycles [26]. These data are subjected to numerical analysis to establish the rate of crack growth, which are stated as a function of ΔK.

The compliance method is another technique for FCG testing, and was carried out according to Annex 5 of ASTM E647-08. As stated in standard, the compliance method is the reciprocal of the force–displacement slope normalized for elastic modulus and specimen thickness [26]. Therefore the relationship between compliance and crack size analytically had been derived for a number of samples.

2.4. Analysis of crack growth rate

From the crack size versus elapsed cycles data (a–N), the crack growth rate da/dN was calculated by following the standard. The crack tip stress intensity factor range, $\Delta K = K_{max} - K_{min}$, was calculated from the maximum and minimum loads of the loading cycles. The fatigue crack growth data was expressed in terms of Paris power-law expression, where the Paris law parameters, C and m, are constants:

$$\frac{da}{dN} = C\Delta K^m \quad (1)$$

3. Results and discussions

3.1. Fatigue crack propagation behavior

The da/dN–ΔK plot generally has three regions; I, II, and III. Regions I and III are the near-threshold and the rapid-crack propagation regions, respectively. Region II is the Paris region, which is defined by a power-law relationship that corresponds to a straight line on a log(da/dN) versus log(ΔK) curve. By using the data reduction technique, as explained in ASTM E647-08, ΔK-increasing can be generated, which corresponds to regions II and III.

The rates of fatigue crack growth for near threshold or ΔK_{th} are extremely slow and large scatter of the data and the influence of pre-cracking conditions make determining the ΔK_{th} value difficult, as it was also found by Motz et al. [6]. Therefore, it is very complicated to experimentally initiate a ΔK-decreasing test, which corresponds to region I [27].

In region III, the crack growth rate is extremely high and obtaining data in this unstable region is quite difficult. For fatigue life prediction, region III is usually disregarded since the number of cycles spent in region III is insignificant compared to the total fatigue life [28]. In this work, regions I and III are not considered.

The ΔK-increasing test was performed and the fatigue crack growth rate or da/dN was attained from the slope of the a–N curve under displacement controlled conditions. Fatigue life in such conditions is very sensitive to the cyclic stress level [29]. The da/dN–ΔK behaviors of porous titanium with and without solid coated surface with load ratios of 0.1 using image processing technique are plotted in Fig. 2. The 60% porous titanium without any coating had a higher Paris exponent ($m = 17.1 \pm 0.3$) than the 60% porous titanium with solid coating ($m = 14.2 \pm 0.2$). The values of m (with one decimal point) were found by curve fitting on experimental data points that have up to 4% maximum experimental error bars, which is below the 5% confidence level.

The parameter C for 60% solid coated porous titanium is 1×10^{-16} and for 60% porous titanium without any coating is 7×10^{-17}. The relationship between C and crack initiation duration is that as C decreases, the crack initiation duration increases [30]. Fig. 2 shows that at a given stress intensity factor, the uncoated specimen had a higher crack growth rate. This means that the porous foam does have a lower fatigue resistance despite a higher m value and lower C value. Both C and m depend on the stress range, mean stress, the material, the test environment, and the details of the testing procedure [31].

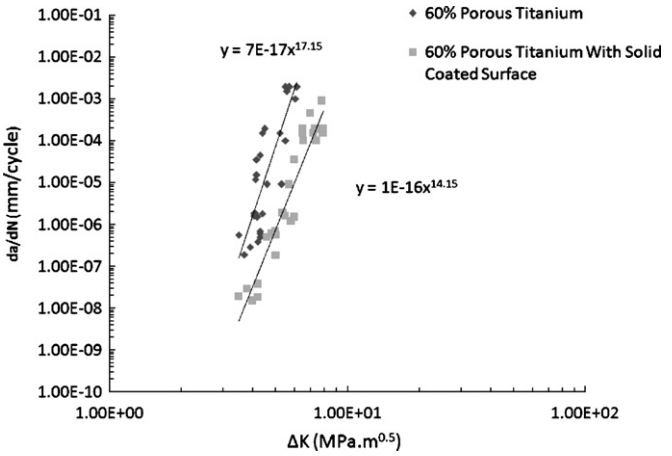

Fig. 2. da/dN–ΔK for 60% porous titanium and 60% porous titanium with solid coated surface at load ratio of 0.1.

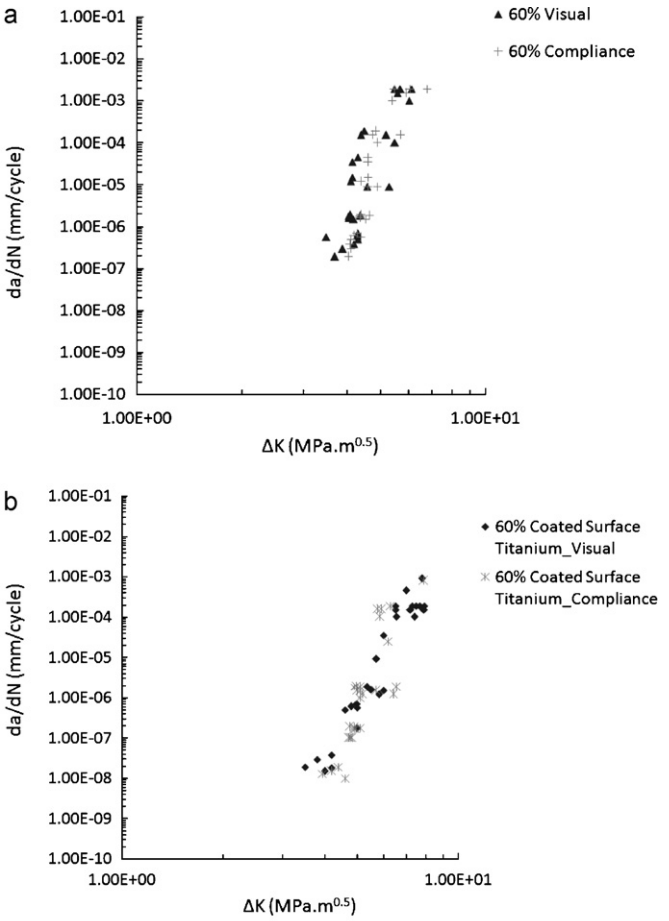

Fig. 3. Comparison of the da/dN–ΔK data using two different techniques (image processing and compliance methods) for 60% porous titanium (a) and 60% porous titanium with solid coated surface (b) at load ratio of 0.1.

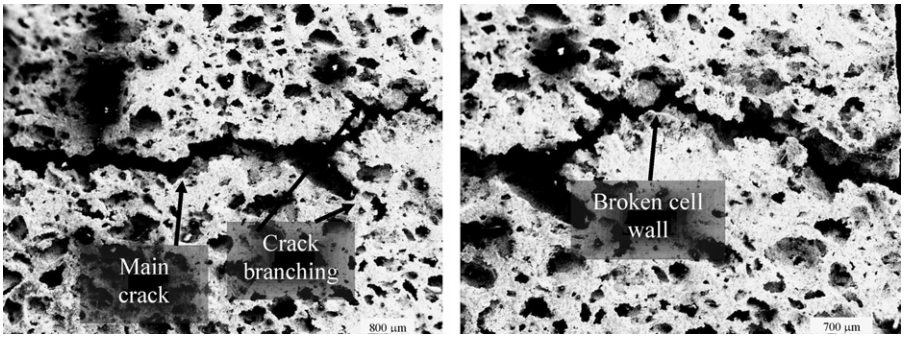

Fig. 4. Scanning electron micrographs (SEM) of the main crack meandering through the cell walls of 60% porous titanium.

The da/dN–ΔK data using the image processing and compliance methods are shown for comparison in Fig. 3a for porous titanium without solid coated surface and in Fig. 3b for solid coated porous titanium at load ratio of 0.1. The experimental difference between the results from the visual and compliance techniques is very small. This suggests the data for da/dN–ΔK measurements at load ratios of 0.1 and 0.5 from visual technique are experimentally verifiable by compliance technique.

3.2. Examination of crack propagation and fracture surface

Crack nucleation is the first stage in the fatigue process and initiates at the highest stress concentration locations. In titanium foams with heterogeneously distributed pores and flaws, the crack nucleation lies at or close to the surface as stress concentration of a near surface defect is higher than the interior defect.

The titanium foam fracture surfaces showed the presence of micro-void coalescence, suggesting that crack advancement was accompanied by ductile deformation in the vicinity of the crack. The ductile micro-void coalescence occurred in thin cell walls due to higher localized stresses versus the normal fatigue fracture surface.

The main crack in the uncoated titanium foam was roughly linear. Fig. 4 shows fatigue crack propagation throughout the heterogeneous porous microstructure, including crack branching resulting in multiple crack tips.

Fig. 5 shows the crack tip and fracture surface for the coated foam, with some ductile tearing of the solid coating evident. Consequently, crack deflection occurred at an angle in the solid coated surface material.

For both coated and uncoated samples, after a certain number of cycles a dominant crack spreads down about the centerline. The crack remained straight throughout some sections of the specimen while following a tortuous path in other sections of the sample, which is due to cracking along the weakest path on tiny cell walls.

The difference between coated and uncoated samples is due to contribution that the thin solid layer has in improving the crack growth resistance. As such, the coated specimen had a higher crack growth resistance for a given stress intensity factor despite the fact that m value was lower and C value was slightly higher than the uncoated samples. Crack initiation started at initial defects such as pre-cracks in the interior sections of the cell walls. Final fracture was seen in regions with low material density or large cells and therefore FCG mostly occurred where cell wall thickness was small. This is in agreement with the results of FCG of aluminum foam by Zettl et al. [7].

3.3. Crack bridging and crack closure

The high Paris exponent in titanium foam can be partially explained by crack bridging and crack closure. Crack bridging and crack closure are both processes that reduce the crack growth rate and therefore extend the fatigue life. Olurin et al. also found a high Paris exponent for Alulight compared to solid ductile metals. They established that the fatigue failure of the cell edges behind the crack tip will cause the degradation of crack bridging and this will control the fatigue crack growth rate [8]. In contrast, the plasticity and increased surface roughness at the crack wake increases the crack bridging and crack closure of the fracture surfaces. The development of crack bridging zone behind the crack tip leads to increase in crack growth resistance as crack progresses.

Crack closure, as was also found in the study by Motz et al. on aluminum foam [6], could be a possible explanation of such high Paris exponent in titanium foams. When the sample goes under tension–tension loading, a plastic zone is created at the crack tip because of the stress concentration. There is also some

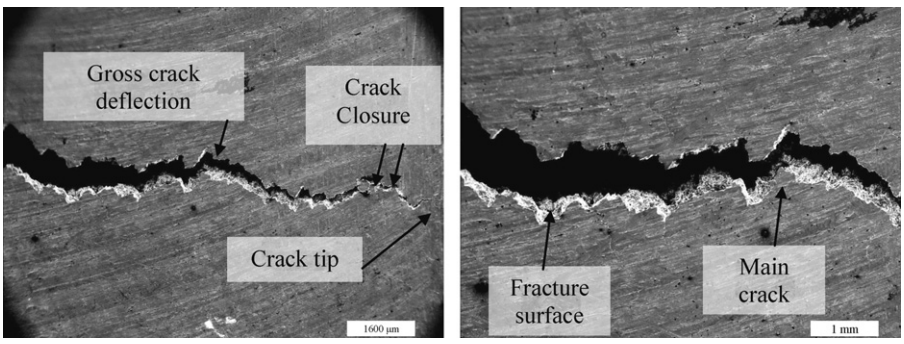

Fig. 5. SEM of the main crack meandering through the cell walls of 60% porous titanium with 0.5 mm solid coated surface, where some ductile tearing is evident.

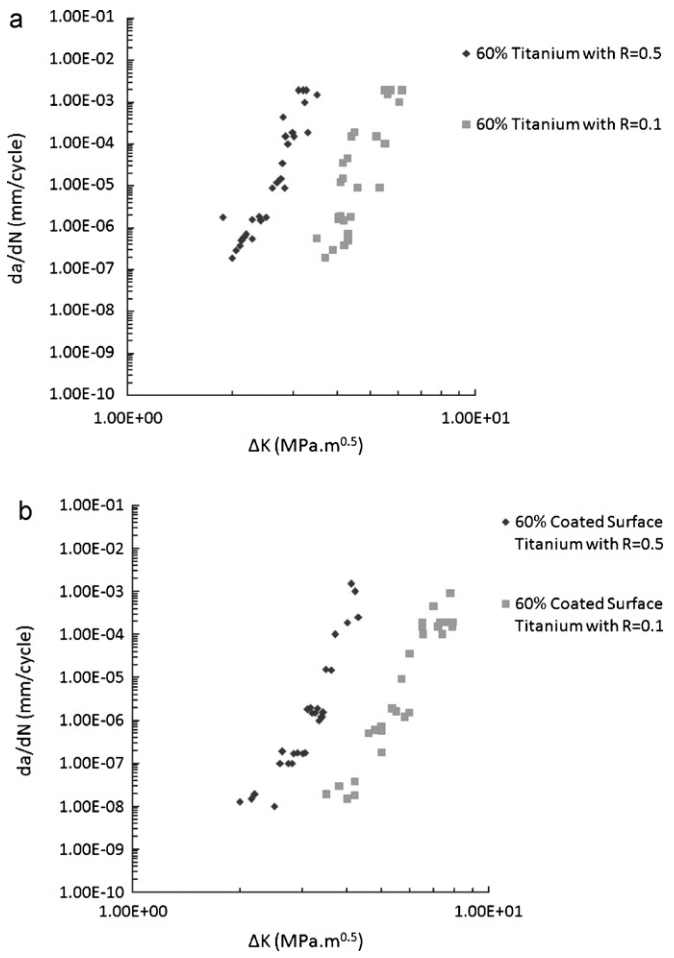

Fig. 6. Plots of da/dN–ΔK for 60% porous titanium (a) and 60% porous titanium with solid coated surface (b) at load ratios of 0.1 and 0.5.

compressive stress as the crack is partly closed till a large tensile stress is applied to stabilize the compressive stress. Therefore, after a certain number of cycles the crack closure occurrence usually vanishes.

3.4. Load ratios

Plots of da/dN–ΔK at load ratios of $R = 0.1$ and $R = 0.5$ for both coated and uncoated titanium foam using the image processing technique are shown in Fig. 6a for 60% porous titanium and in Fig. 6b for solid coated titanium foam. According to Paris law (Eq. (1)), the fatigue crack propagation only depends on ΔK, and it is insensitive to the load ratio in region II (Fig. 6) [32]. There are other proposed relationships such as Forman [32] that will take into account the sensitivity of da/dN to load ratio. However, in addition to region II, data from either of region I or III, or all of the sigmoidal da/dN–ΔK relationship must be considered in these empirical equations. In this study, only region II of da/dN–ΔK curve

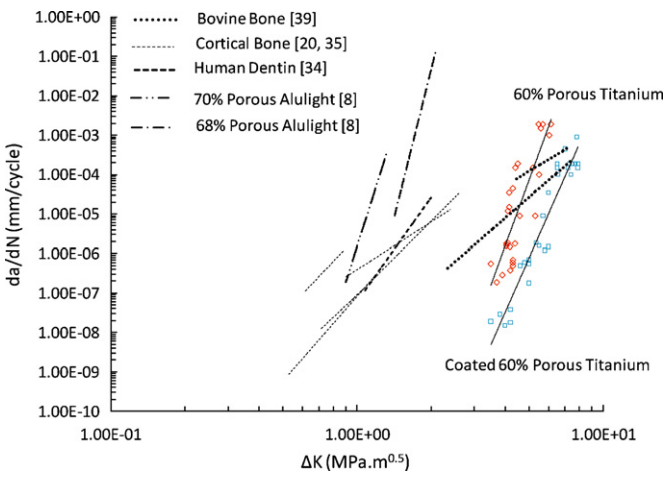

Fig. 7. Comparison of the da/dN–ΔK data of different materials.

has been plotted (Fig. 6). The Paris exponent m is slightly higher for uncoated titanium foam at load ratio of 0.1 ($m = 17.15$) than load ratio of 0.5 ($m = 16.59$). In contrast the Paris exponent m is a little lower for coated titanium foam at load ratio of 0.1 ($m = 14.16$) than at load ratio of 0.5 ($m = 15.76$). The load ratio had a negligible effect on the FCG behavior of both materials.

3.5. Disadvantages of coating titanium foams for biomedical applications

The manufacturing method used in this paper to create the solid coated surface is only limited to simple plate and regular surfaces and cannot be used for complex shapes. The coating did increase the fatigue crack growth resistance for higher values of ΔK, however, the lower Paris exponent, m, and higher fatigue crack coefficient, C, meant that this difference was not as significant at lower values of ΔK. The presence of the coating has other drawbacks when used for metal implants, including reduction of space available for bone ingrowth as well as potential degradation of the coating material [16].

3.6. Comparison of fatigue crack growth rate to different materials

Paris law parameters, m and C, which are experimentally determined scaling constants, are shown in Table 1 for the titanium foams used in this study, as well as literature values for solid titanium and some common skeletal parts. The C values for porous material are recorded to be lower than pure titanium solid ($C = 1.95 \times 10^{-11}$) [33], dentine ($C = 6.24 \times 10^{-11}$) [34], and cortical bone ($6.5 \times 10^{-8} < C < 3.7 \times 10^{-6}$) [20,35].

The Paris exponent (m) of titanium foam with 60% porosity is significantly higher than the Paris exponent of 3.41 for solid titanium. Foam materials with significantly higher m values than solid metals are less at risk of failure by crack growth propagation [36] due to the crack bridging and closure mechanisms. The Paris expo-

Table 1
Comparison of Paris exponents for different materials.

Material	m	C	References
Pure titanium	3.41	1.95×10^{-11}	[33]
Dentine	8.76	6.24×10^{-11}	[34]
Cortical bone	$4.4 < m < 9.5$	$6.5 \times 10^{-8} < C < 3.7 \times 10^{-6}$	[20,35]
60% Solid Coated porous titanium	14.16	1×10^{-16}	
60% Porous titanium	17.15	7×10^{-17}	

nents of metal foams are reported to be considerably higher than solid metals, nonetheless much lower than the Paris exponent of ceramics that are as high as 50 and above [37,38]. Ceramics have pores and microcracks and such high Paris exponents in ceramics may possibly be due to crack closure, debris, or even microcracking and microplasticity [38]. Alulight with comparable porosity to titanium foams also have similarly high Paris exponent values (19.66 for 70% Alulight and 24.98 for 68% Alulight) [8].

The Paris exponent for cortical bone (4.4–9.5) and dentine (8.76) are also recorded to be lower than 60% titanium foams [20,35]. Fig. 7 shows that at a given ΔK, bovine bones [39] have a comparable FCG resistance as uncoated titanium foam. Conversely, the Paris exponent of bovine bones recorded to be $3.71 < m < 5.42$, which is much lower than uncoated titanium foam. Elastic strain concentration at the tip of the crack shown to be the main factor in FCG in metallic foams; nevertheless bovine bones or bones in general, do not show to act in accordance with such frequent behavior found in metallic foams.

High porous titanium foams have a good fatigue crack growth resistance and may be used as cancellous bone and dentine in orthopaedic and dental applications. Even though the titanium foams have seen to have reasonable crack growth resistance rate as biomaterial, this property may improve by maintaining the purity of titanium powder during the foam making process, which leads to better mechanical properties.

4. Conclusions

The following conclusions can be drawn from this study:

- Titanium foam with 60% porosity has a significantly higher Paris exponent than solid titanium, most likely caused by crack closure and crack bridging. The Paris exponent was also higher than cortical bone and dentine, suggesting that high porous titanium foams would not be limited by their fatigue crack growth resistance for implantation at various skeleton parts.
- The results of mode I fatigue crack growth of titanium foams are in good agreement from both reproducible image processing and compliance techniques.
- A solid coating on the titanium foam resulted in lower crack growth rates for a given stress intensity factor, and a lower Paris exponent than the uncoated foam.
- The load ratio had a negligible effect on the FCG behavior of both materials in region II, which agrees with Paris law.

Acknowledgements

This work is financially supported by the Australian Research Council (project no: DP0770021) and ARC grant from ARNAM. The authors also thank David Dick for his support in the E-CORE laboratory at the University of Toledo, Ohio.

References

[1] S. Kashef, A. Asgari, T. Hilditch, W. Yan, V.K. Goel, P.D. Hodgson, Mater. Sci. Eng. A 527 (29–30) (2010) 7689–7693.
[2] B.P. Boden, M.J. Matava, Stress Fractures, Soc.Sports Med. (2008).
[3] J.J. Kruzic, J.A. Scott, R.K. Nalla, R.O. Ritchie, J. Biomech. 39 (2006) 968–972.
[4] D.B. Burr, Bone Exerc. Stress Fract. Exerc Sport Sci. Rev. (1997).
[5] C.E. Wen, Y. Yamada, A. Nouri, P.D. Hodgson, Mater. Sci. Forum 539–543 (2007) 720–725.
[6] C. Motz, O. Friedl, R. Pippan, Int. J. Fatigue 27 (2005) 1571–1581.
[7] B. Zettl, H. Mayer, S.E. Stanzl-Tschegg, H.P. Degischer, Mater. Sci. Eng. A 292 (1) (2000) 1–7.
[8] O.B. Olurin, K.Y.G. McCullough, N.A. Fleck, M.F. Ashby, Int. J. Fatigue 23 (2000) 375–382.
[9] K.Y.G. McCullough, N.A. Fleck, M.F. Ashby, Acta Mater. 47 (8) (1999) 2331–2343.
[10] S. Thelen, F. Barthelat, L.C. Brinson, J. Biomed. Mater. Res. A 69A (4) (2004) 601–610.
[11] H. Li, S.M. Oppenheimer, S.I. Stupp, D.C. Dunand, L.C. Brinson, Mater. Trans. – JIM 45 (2004) 1124–1131.
[12] M. Takemoto, S. Fujibayashi, M. Neo, J. Suzuki, T. Kodubo, T. Nakamura, Biomaterials 26 (2005) 6014–6023.
[13] Y. Chino, D.C. Dunand, Acta Mater. 56 (2008) 105–113.
[14] A. Schuh, J. Luyten, R. Vidael, W. Honle, T. Schmickal, Mater. Sci. Eng. Technol. 38 (12) (2007).
[15] Z. Esen, S. Bor, Scripta Mater. 56 (2007) 341–344.
[16] C.E. Wen, Y. Yamada, K. Shimojima, Y. Chino, H. Hosokawa, M. Mabuchi, J. Mater. Res. 17 (10) (2002) 2633–2639.
[17] T. Imwinkelried, J. Biomed. Mater. Res. A (2007) 964–970.
[18] S.H. Teoh, R. Thampuran, W.K.H. Seah, J.C.H. Goh, Biomaterials 14 (6) (1993) 407–412.
[19] N.G. Davis, J. Teisen, C. Schuh, D.C. Dunand, J. Mater. Res. 16 (5) (2001) 1508–1518.
[20] R.K. Nalla, J.J. Kruzic, J.H. Kinney, R.O. Ritchie, Biomaterials 26 (2005) 2183–2195.
[21] S. Kashef, W. Yan, J. Lin, P.D. Hodgson, Modern Phys. Lett. B 22 (2008) 6155–6160.
[22] D.P. Byrne, D. Lacroix, J.A. Planell, D.J. Kelly, P.J. Prendergast, Biomaterials 28 (2007) 5544–5554.
[23] M. Bram, H. Schiefer, D. Bogdanski, M. Koller, H.P. Buchkremer, D. Stover, Metal Powder Rep. 61 (2006) 26–31.
[24] K. Ishizaki, S. Komarneni, M. Nanko, Porous Materials, Process Technology and Applications, Kluwer Academic Publishers, Dordrecht, The Netherlands, 1998.
[25] A.H. Noroozi, G. Glinka, S. Lambert, Int. J. Fatigue 27 (2005) 1277–1296.
[26] ASTM E647-08, Standard Test Method for Measurement of Fatigue Crack Growth Rates, ASTM International, West Conshohocken, PA, 2008.
[27] R.I. Stephens, A. Fatemi, R.R. Stephens, H.O. Fuchs, Metal Fatigue in Engineering, second ed, Wiley-Interscience, New York, 2001.
[28] S.K. As, Fatigue Life Prediction of an Aluminum Alloy Automotive Component Using Finite Element Analysis of Surface Topography, Trondheim, Norway, Norwegian University of Science and Technology, 2006.
[29] K.H.J. Buschow, R. Cahn, M. Flemings, B. Ilschner, E. Kramer, S. Mahajan, P. Veyssiere, Encyclopedia of Materials: Science and Technology, Elsevier, 2001.
[30] M. Bizeul, C. Bouvet, J.J. Barrau, R. Cuenca, Int. J. Fatigue 32 (2010) 60–65.
[31] O.G. Bilir, Eng. Fract. Mech. 36 (2) (1990) 361–364.
[32] T.L. Anderson, Fracture Mechanics: Fundamentals and Applications, CRC Press, 1995.
[33] A. Carpinteri, M. Paggi, Frattura ed Integrita Strutturale 2 (2007) 10–16.
[34] R.K. Nalla, V. Imbeni, J.H. Kinney, S.J. Marshall, R.O. Ritchie, On the Development of Life Prediction Methodologies for the Failure of Human Teeth, 2002.
[35] R.O. Ritchie, J.H. Kinney, J.J. Kruzic, R.K. Nalla, Fatigue Fract. Eng. Mater. Struct. 28 (2005) 345–371.
[36] S.K. Obwoya, T. Baker, W. Soboyejo, Mater. Manuf. Process. 22 (2007) 206–213.
[37] S. Suresh, Fatigue of Materials, Cambridge University Press, Great Britain, 1991.
[38] S. Li, L. Sun, W. Jia, Z. Wang, J. Mater. Sci. Lett. 14 (1995) 1493–1495.
[39] T.M. Wright, W.C. Hayes, J. Biomed. Mater. Res. 10 (1976) 637–648.